Hydrogen-rich scandium compounds at high pressures

Kazutaka Abe
Research Institute of Electrical Communication, Tohoku University, 2-1-1 Katahira, Aoba, Sendai, Miyagi 980-8577, Japan
(Received 25 November 2016; published 16 October 2017)

Scandium hydrides at high pressures have been investigated by using *ab initio* density functional calculations. Although the stable scandium hydride so far known to have the highest content rate of hydrogen is ScH_3, other more hydrogen-rich compounds are found to be possible at high pressures. These are ScH_4 in the $I4/mmm$ structure above 160 GPa, ScH_6 in the $P6_3/mmc$ structure from 135 to 265 GPa, and ScH_6 in the $Im\bar{3}m$ structure above 265 GPa. The three phases are all metallic, and the superconducting transition temperatures estimated from the extended McMillan equation are 67 K in the $I4/mmm$ ScH_4 at 195 GPa, 63 K in the $P6_3/mmc$ ScH_6 at 145 GPa, and 130 K in the $Im\bar{3}m$ ScH_6 at 285 GPa. While the $I4/mmm$ tetrahydride and the $Im\bar{3}m$ hexahydride were similarly predicted for yttrium (another group-3 element), the $P6_3/mmc$ hexahydride is possible only for scandium. The smaller atomic size of scandium stabilizes the $P6_3/mmc$ structure, and other nearby d-block elements, whose atomic sizes are smaller or comparable, might be likewise capable of forming such polyhydrides.

DOI: 10.1103/PhysRevB.96.144108

I. INTRODUCTION

After the prediction of high-temperature superconductivity in dense metallic hydrogen by Ashcroft [1], Gilman pointed out that the same mechanism of superconductivity is also applicable to metallic hydrides which can be achieved at much lower pressures [2]. The idea was revived about a decade ago [3,4], chief attention being paid to hydrogen-rich compounds such as group-14 hydrides. Since then, compressed hydrides have been drawing interest considerably in high pressure physics and investigated extensively both in experiment [5–10] and in theory [11–22]. Recently, there was a noticeable experimental observation that dense sulfur hydride leads to high-temperature superconductivity, where the transition temperature (T_c) is 203 K at 155 GPa [8]. Actually, for sulfur hydride, high-temperature superconductivity had been already predicted from theory: $T_c \sim 80$ K for SH_2 [20] and $T_c \sim 200$ K for SH_3 [21]. A recent experiment claimed that the superconducting phase at 155 GPa has the composition of SH_3 [9], but it is still controversial which kind of compound brings about the high value of T_c [10].

A curious aspect of high compression is that it often allows substances to take up more hydrogen than ambient pressure does. In particular, many metallic polyhydrides have been proposed for alkaline and alkaline-earth elements at high pressures [23–32]. The trend is also suggested for one of the group-3 elements, namely, yttrium as pointed out by Li *et al.* [33]. They showed that YH_4 and YH_6 are stabilized with $I4/mmm$ and $Im\bar{3}m$ symmetries, respectively, above 110 GPa. The estimated values of T_c at 120 GPa are 84 K for the $I4/mmm$ YH_4 and 251 K for the $Im\bar{3}m$ YH_6 with Coulomb pseudopotential $\mu^* = 0.13$. Intriguingly, the $I4/mmm$ and $Im\bar{3}m$ structures were also proposed for CaH_4 and CaH_6, respectively, by Wang *et al.* [26]. While the density of states (DOS) at the Fermi energy is very small in the $I4/mmm$ CaH_4, the $Im\bar{3}m$ CaH_6 is a good metal and has a high value of T_c which exceeds 200 K. The high-T_c $Im\bar{3}m$ phase was further predicted with respect to MgH_6, though the phase is stabilized only above 325 GPa [32]. These theoretical findings tempt one to look into scandium, which is located close to yttrium, calcium, and magnesium on the periodic table. Moreover, it is very interesting to investigate whether the tendency to form metallic polyhydrides is extensively found even in the d block. Thus, as the first d-block element, scandium is selected in this paper, and its hydrides are examined by using *ab initio* methods.

Around one atmosphere, scandium dihydride can exist as a stable phase, which has the CaF_2-type structure [34,35]. When pressure is increased to 0.3 GPa, the synthesis of scandium trihydride becomes possible [36,37]. According to neutron diffraction measurements [38], the composition is close to $ScH_{2.9}$, and the structure is hexagonal with $P6_3/mmc$ symmetry, where half of the 4e sites are randomly occupied such that no H atoms come too close to each other. At higher pressures, fcc trihydride is eventually stabilized [39,40]: Specifically, the hexagonal phase is firstly transformed into an intermediate phase at 25 GPa, and then the intermediate phase into the fcc phase at 46 GPa. All the phases mentioned above (i.e., the CaF_2-type dihydride and the hexagonal, intermediate, and fcc trihydrides) are likewise observed in yttrium hydrides, though there is a little structural difference in the hexagonal trihydrides. These facts might seem to indicate that the similarity persists to higher pressures. Yet, contrary to expectations, *ab initio* calculations performed here have predicted a new high-pressure phase of ScH_6 with $P6_3/mmc$ symmetry, which is not stabilized in YH_6. The $P6_3/mmc$ ScH_6 is metallic, and its T_c reaches ~60 K. If the $P6_3/mmc$ hexahydride or its close modification is possible for other d-block elements, even higher T_c might be expected as a result of the shift of the Fermi energy caused by the increase of the valence electron number.

II. TECHNICAL DETAILS

A. Computational conditions

The first-principles calculations presented in this paper are based on the density functional theory within the generalized gradient approximation [41]. The computations are carried out by using QUANTUM ESPRESSO [42], which utilizes plane-wave basis sets and ultrasoft pseudopotentials [43]. The cutoff radii of the pseudopotentials are 0.794 Å for Sc (with $1s2s2p$ as core) and 0.423 Å for H, and the cutoff energy is set at 816 eV.

For the calculations of enthalpy, the k-point number is chosen to be about $(40\ \text{Å})^3/v_{\text{cell}}$, where v_{cell} is the volume of the unit cell. A Fermi-distribution smearing is used with a temperature of $k_B T = 0.1$ eV.

The calculations of electron-phonon interaction are performed by using the density functional perturbation theory [44]. Regarding the analyses of the electron-phonon coupling, the numbers of k points and q points (phonon wave vectors) are taken to be about $(50\ \text{Å})^3/v_{\text{cell}}$ and $(13\ \text{Å})^3/v_{\text{cell}}$, respectively.

B. Structural search method

Stable structures are searched simply by trying various structures in a random manner, which is analogous to the method outlined in Refs. [11] and [45], as described below. Firstly, an initial structure is generated randomly for a target system designated with v_{cell} and the numbers of Sc and H atoms in the unit cell. Then, the structural optimization is carried out with v_{cell} fixed. This procedure is repeated until a structure which is likely to be the most stable is encountered at least a few times. Throughout this random search process, the k-point number is set at about $(20\ \text{Å})^3/v_{\text{cell}}$, and the cutoff energy is set at 585 eV. Then, after the search process is ended, several low-energy structures are selected and refined with the larger k-point number [$\sim(40\ \text{Å})^3/v_{\text{cell}}$] and the higher cutoff energy (816 eV).

The following restrictions are enforced on initial structural parameters: (1) The lengths of lattice vectors (a,b,c) satisfy $L \leqslant a,b,c \leqslant 3L$ where L is determined to give the required v_{cell}; (2) the angles of lattice vectors (α,β,γ) satisfy $40^\circ \leqslant \alpha,\beta,\gamma \leqslant 140^\circ$; (3) Sc-Sc, Sc-H, H-H distances are larger than 1.98, 1.52, and 1.06 Å, respectively. Regarding restriction (2), it should be noted that the angles can always be transformed into the values between 60° and 120° by making use of the freedom in choosing lattice vectors. In restriction (3), each of the minimum distances is set to be 1.25 times as large as the sum of the pseudopotential radii. These distances might look a little too large as minimum distances. However, such a setting is really useful because it has an effect of distributing atoms evenly within the unit cell.

Several examples of the structural searches are shown in Table I, where the results of ScH_4 and ScH_6 (which are stable compositions as will be discussed later) are presented. The efficiency of the searches can be known from the ratio $N_{\text{stable}}/N_{\text{tot}}$, where N_{stable} is the number of times the stable structure is encountered, and N_{tot} is the total number of generated structures. It turns out to be quite easy to find out the stable structure of ScH_4, which has $I4/mmm$ symmetry; remarkably, $N_{\text{stable}}/N_{\text{tot}}$ is larger than 0.1 even for the unit cell with four formula units (20 atoms). Contrarily, the searches of ScH_6 phases are more complicated. When the unit cell contains four formula units (28 atoms), the values of $N_{\text{stable}}/N_{\text{tot}}$ are about 0.001 for both of the $P6_3/mmc$ and $Im\bar{3}m$ structures. These figures of $N_{\text{stable}}/N_{\text{tot}}$ for ScH_4 and ScH_6 indicate that the sufficient size of N_{tot} strongly depends on what system is investigated.

To further evaluate the validity of the search method, it is additionally applied to dense hydrogen as presented in Table I [47]. Within the clamped nuclei approximation, the stable structure of H at 410 GPa is the $Cmca$ structure [48] (molecular phase) and that at 515 GPa is the $Fddd$ structure [49,50] (atomic phase) which is obtained by slightly deforming the Cs-IV ($I4_1/amd$) structure [51]. The present method has succeeded in finding out both the structures. As clearly seen, the search of the molecular phase (where $N_{\text{stable}}/N_{\text{tot}} = 0.020$) is more difficult than that of the atomic phase (where $N_{\text{stable}}/N_{\text{tot}} = 0.033$). Nonetheless, even for the molecular phase, N_{tot} of a few hundred is large enough for the unit cell consisting of 16 atoms to be examined.

TABLE I. Efficiency of the random structural searches for ScH_4, ScH_6, and H. Here, n_{atom} is the number of atoms in the unit cell, N_{stable} the number of times the structure which is stable (or metastable if the system should be inhomogeneous at the density) encountered, and N_{tot} the total number of structures generated randomly. See Ref. [46] for the definition of r_s. The pressures are those obtained within the clamped nuclei approximation.

	r_s	P (GPa)	Structure	n_{atom}	N_{stable}	N_{tot}	$\frac{N_{\text{stable}}}{N_{\text{tot}}}$
ScH_4	1.54	196	$I4/mmm$	5	339	485	0.70
				10	254	527	0.48
				20	82	652	0.13
ScH_6	1.52	190	$P6_3/mmc$	14	25	2348	0.011
				28	6	5452	0.0011
	1.43	305	$Im\bar{3}m$	7	75	842	0.089
				14	29	1820	0.016
				28	8	6517	0.0012
H	1.27	410	$Cmca$	16	43	2191	0.020
	1.22	515	$Fddd$	16	65	1970	0.033

III. STABLE STRUCTURES

The random structural searches have been carried out for three compositions, namely, ScH_4, ScH_5, and ScH_6 at the densities corresponding to ~200 GPa. For each composition, unit cells are set to contain at most four formula units. This choice of the cell size is considered to be reasonable because most of stable hydrides so far proposed from theory have no more than four formula units in the primitive cell, especially when the compound is very hydrogen-rich (i.e., XH_n with $n > 3$) or when pressure is higher than ~120 GPa. The structural searches have predicted that candidate structures of ScH_4, ScH_5, and ScH_6 have $I4/mmm$, $C2/m$, and $P6_3/mmc$ symmetries, respectively. As mentioned earlier, the $I4/mmm$ structure is also the stable structure of YH_4 [33] and CaH_4 [26]. On the other hand, the $P6_3/mmc$ structure is not stabilized in YH_6 and CaH_6, which instead take the $Im\bar{3}m$ structure [26,33]. Actually, the appearance of the $Im\bar{3}m$ structure in ScH_6 requires more compression; the transition from the $P6_3/mmc$ ScH_6 to the $Im\bar{3}m$ ScH_6 is estimated to take place at 325 (265) GPa for a static (dynamic) ionic system.

The $P6_3/mmc$ structure is less packed and less isotropic than the $Im\bar{3}m$ structure. Each Sc atom is surrounded by 18 H atoms in the $P6_3/mmc$ structure (where two kinds of Sc-H distances exist) while by 24 H atoms in the $Im\bar{3}m$ structure. The stability of the $P6_3/mmc$ structure is thus caused by the smaller atomic size of scandium, which leads to significant overlap of Sc and H orbitals. As a matter of fact, also in MgH_6, the $P6_3/mmc$ structure has lower enthalpy than the $Im\bar{3}m$ structure up to about 330 (230) GPa for a

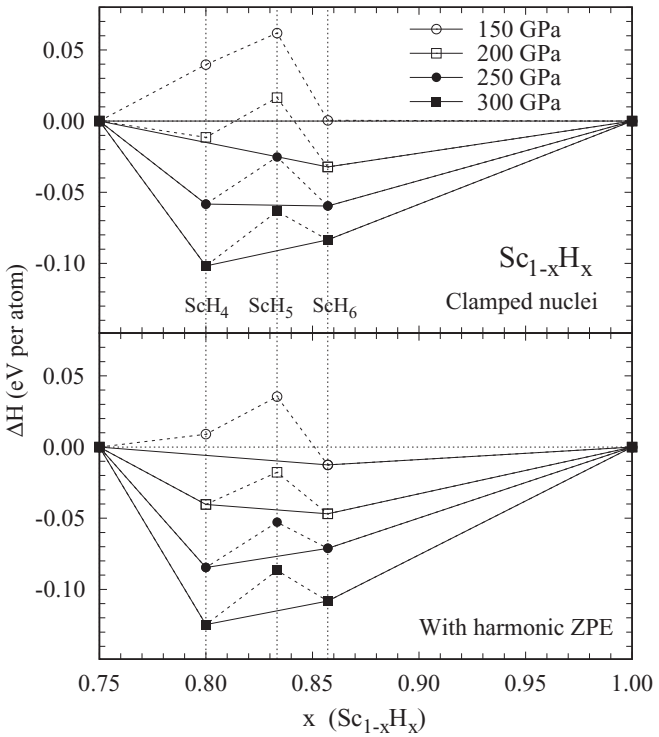

FIG. 1. Enthalpy per atom of $Sc_{1-x}H_x$ as a function of x. The enthalpy is given relative to that of the system consisting of ScH_3 and H phases. In the top (bottom) panel, the ionic system is treated as a static (dynamic) one. The ScH_4 has $I4/mmm$ symmetry; the ScH_5 has $C2/m$ symmetry; the ScH_6 has $P6_3/mmc$ symmetry below 325 (265) GPa and $Im\bar{3}m$ symmetry above 325 (265) GPa for the static (dynamic) ionic system. The enthalpy of ScH_3 is calculated for the $Fm\bar{3}m$ structure [39], and that of H for the $C2/c$ [54], the $Cmca$-12 [54], the $Cmca$ [48], and the Cs-IV ($I4_1/amd$) [51] structures. As a guide to the eye, stable phases are connected with solid lines.

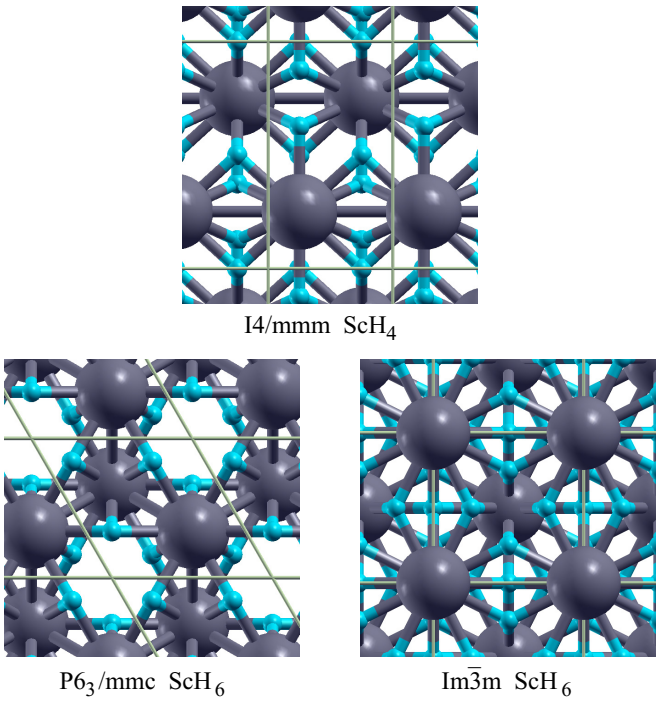

FIG. 2. The $I4/mmm$ structure for ScH_4 (above 160 GPa), the $P6_3/mmc$ structure for ScH_6 (from 135 to 265 GPa), and the $Im\bar{3}m$ structure for ScH_6 (above 265 GPa). The detailed structural parameters are as follows. The $I4/mmm$ ScH_4 (195 GPa): $a = 2.605$ Å, $c = 4.767$ Å; Sc at 2b sites (0, 0, 1/2); H at 4d sites (0, 1/2, 1/4) and 4e sites (0, 0, 0.125). The $P6_3/mmc$ ScH_6 (145 GPa) : $a = 3.419$ Å, $c = 4.271$ Å; Sc at 2c sites (1/3, 2/3, 1/4); H at 12k sites (0.166, 0.332, 0.630). The $Im\bar{3}m$ ScH_6 (285 GPa): $a = 3.242$ Å; Sc at 2a sites (0, 0, 0); H at 12d sites (1/4, 0, 1/2).

static (dynamic) ionic system. (But, note that MgH_6 itself is unstable to decomposition into MgH_4 and H at the pressures [32].) The tendency is clearly observed when the enthalpies of the $P6_3/mmc$ and $Im\bar{3}m$ hexahydrides are compared for Mg, Ca, Sc, Y, Ti, Zr, and so on. For example, for Ca (1.76 Å), Sc (1.70 Å), Ti (1.60 Å), and V (1.53 Å), where the figures in the parentheses are their covalent radii [52], the $P6_3/mmc$ hexahydride has lower enthalpy than the $Im\bar{3}m$ one up to 55, 325, 555, and 677 GPa (for a static lattice), respectively. The structural resemblance between MgH_6 and ScH_6 also suggests the existence of a diagonal relationship: the similarity in chemical properties between diagonally adjacent elements [53]. Indeed, calcium and yttrium are likewise diagonally adjacent and show the aforementioned structural resemblance in dense polyhydrides. Furthermore, such a similarity was found between aluminum and germanium. While AlH_3 takes the $Pm\bar{3}n$ (A15) structure at high pressures [5,12], GeH_3 is stabilized in the $Cccm$ structure which is very close to the $Pm\bar{3}n$ structure [19]. Although the origin of the diagonal relationship has not been completely understood yet [53], this rule can serve as a practical clue in looking for other similar metallic hydrides. In particular, the rule is useful in controlling the position of the Fermi energy since diagonally adjacent elements have different valence electron numbers [19].

It is then checked whether ScH_4, ScH_5, and ScH_6 are stable to decomposition. In Fig. 1, the enthalpy per atom of $Sc_{1-x}H_x$ is shown as a function of x. The enthalpy is given relative to that of the decomposed system which comprises ScH_3 ($Fm\bar{3}m$) and H phases. This choice of the reference system simply comes from the theoretical findings that ScH_3 is quite stable to decomposition and takes $Fm\bar{3}m$ symmetry up to about 360 GPa [55]. The x dependence of enthalpy shows that ScH_4 and ScH_6 are possible while ScH_5 is unstable all over the pressures considered here. The effects of zero-point energy (ZPE) of nuclei on decomposition are also examined, where the ZPE is calculated from the frozen-phonon method by using the Phonopy code [56]. The numbers of atoms in the supercells used for the frozen-phonon calculations are 96 or 128 for H, 128 for the $Fm\bar{3}m$ ScH_3, 80 for the $I4/mmm$ ScH_4, 96 for the $C2/m$ ScH_5, and 112 for the $P6_3/mmc$ and $Im\bar{3}m$ ScH_6. With the ZPE considered, the $I4/mmm$ ScH_4 is stabilized above 160 GPa, the $P6_3/mmc$ ScH_6 from 135 to 265 GPa, and the $Im\bar{3}m$ ScH_6 above 265 GPa.

The stable structures thus obtained for ScH_4 and ScH_6 are illustrated in Fig. 2. All three structures have no tight H pairs. The closest H-H distances are 1.196 Å in the $I4/mmm$ ScH_4 at 195 GPa, 1.025 Å in the $P6_3/mmc$ ScH_6 at 145 GPa, and 1.146 Å in the $Im\bar{3}m$ at 285 GPa. This structural property is actually another implication that the systems are stable to decomposition. In the $P6_3/mmc$ ScH_6, a hexagonal void space

along the c axis is somewhat prominent. The presence of the space might prompt one to think that it could be filled with more H atoms. The possibility was in fact investigated by considering ScH_7 and ScH_8, and the calculations showed that such structures are unstable to decomposition into ScH_6 and H.

IV. ELECTRONIC STRUCTURES

The projected DOS (PDOS) is displayed in Fig. 3, and all the phases proposed here are found to be metallic. For comparison, the PDOS of the $Fm\bar{3}m$ ScH_3 is also presented [Fig. 3(a)]. The $Fm\bar{3}m$ ScH_3 was predicted to be metallic from theory [55,57], which is consistent with experimental observations for fcc ScH_3 around 50 GPa [40]. In spite of the metallic properties of the $Fm\bar{3}m$ ScH_3, the electronic structures are not suitable for increasing T_c [57]. The Fermi energy lies just on the edge of the sharp peaks chiefly consisting of localized Sc $3d$ states. Moreover, the contribution of H orbitals to the DOS is quite small at the Fermi energy, indicating that electron-phonon coupling is weak with respect to high frequency phonons. These features remain almost unchanged at higher pressures although the $3d$ peaks become a little less sharp. In contrast, in the ScH_4 and ScH_6 phases, significant contributions of H orbitals to the DOS are observed at the Fermi energy. As a result of the Sc-H hybridization, the bands crossing the Fermi energy are steep in comparison with those in the ScH_3 phase. The dispersive character is particularly prominent in the $Im\bar{3}m$ ScH_6 as already found for YH_6, CaH_6, and MgH_6 in the $Im\bar{3}m$ structure [26,32,33].

Now, it is worthwhile to compare the DOS of the scandium, yttrium, and calcium hydrides (Fig. 4); by way of addition, the DOS of the $P6_3/mmc$ YH_6 and CaH_6 are also shown even though these phases are unstable. One of the clear differences between scandium and yttrium is that the DOS just above the Fermi energy is larger in the scandium hydrides than in the yttrium hydrides. This property is apparently attributable to the localized nature of Sc $3d$ orbitals. On the other hand, around and just below the Fermi energy, the DOS curves of the scandium hydrides are similar to those of the yttrium hydrides. The similarity still holds for the $P6_3/mmc$ phases, though the $P6_3/mmc$ YH_6 is unstable.

The calcium hydrides exhibit the shift of the Fermi energy which stems from the smaller number of valence electrons. In the $I4/mmm$ CaH_4, in addition to the shift of the Fermi energy, the shape of the DOS is distinctly changed from those of the scandium and yttrium hydrides. The change of the DOS shape is also observed in the $P6_3/mmc$ CaH_6, though it is to a lesser extent. However, in the $Im\bar{3}m$ phase, the rigid band model seems to be a fairly good approximation, especially when CaH_6 is compared with YH_6. This feature again indicates that the $Im\bar{3}m$ structure has rather delocalized electronic properties. The DOS at the Fermi energy in the $Im\bar{3}m$ CaH_6 is a little lower than those in the $Im\bar{3}m$ ScH_6 and YH_6 owing to the shift of the Fermi energy. Yet, it is worth mentioning that the H contributions to the DOS at the Fermi energy, which are crucial to high T_c, are almost the same size for all three $Im\bar{3}m$ hexahydrides. This is in fact understood from the shape of the PDOS of H atoms in Fig. 3(d).

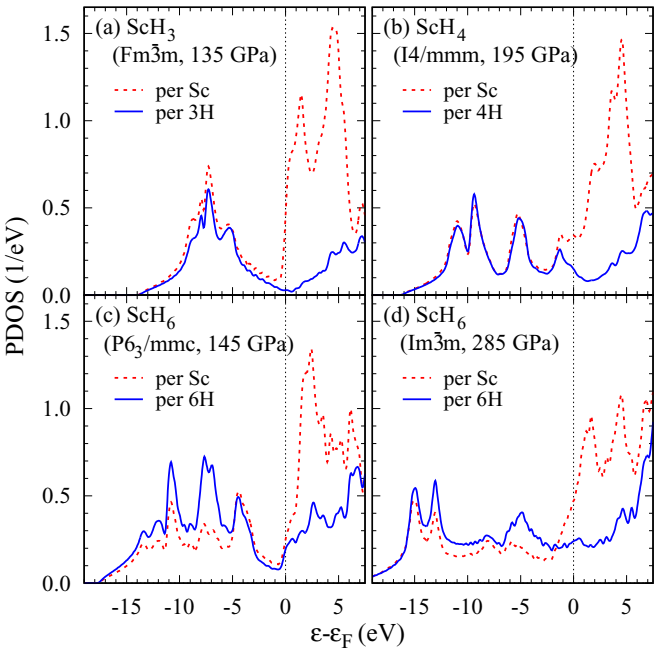

FIG. 3. DOS projected onto each element: (a) the $Fm\bar{3}m$ ScH_3 at $r_s = 1.65$ (135 GPa); (b) the $I4/mmm$ ScH_4 at $r_s = 1.55$ (195 GPa); (c) the $P6_3/mmc$ ScH_6 at $r_s = 1.57$ (145 GPa); (d) the $Im\bar{3}m$ ScH_6 at $r_s = 1.45$ (285 GPa).

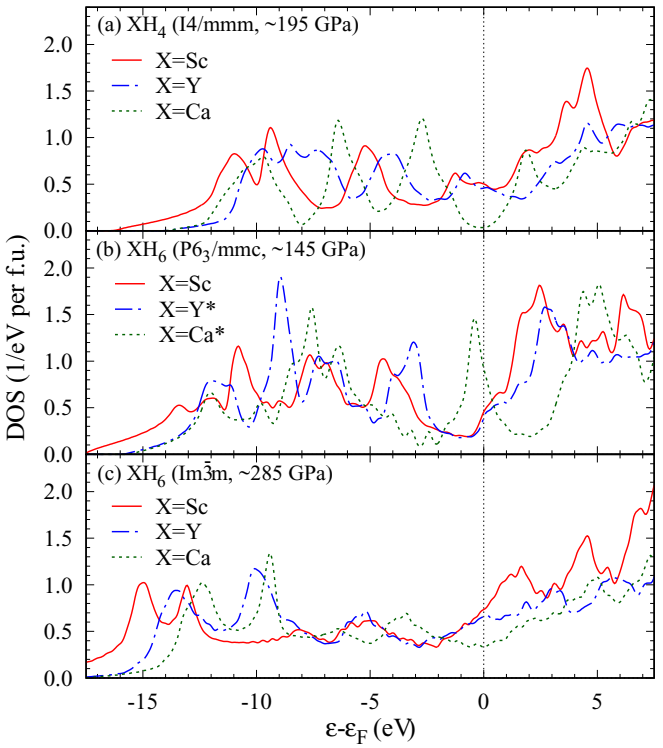

FIG. 4. Total DOS of scandium hydrides in comparison with those of yttrium and calcium hydrides: (a) the $I4/mmm$ tetrahydrides at ~195 GPa; (b) the $P6_3/mmc$ hexahydrides at ~145 GPa; (c) the $Im\bar{3}m$ hexahydrides at ~285 GPa. The asterisks mean that the phases are unstable all over the pressure regime considered here.

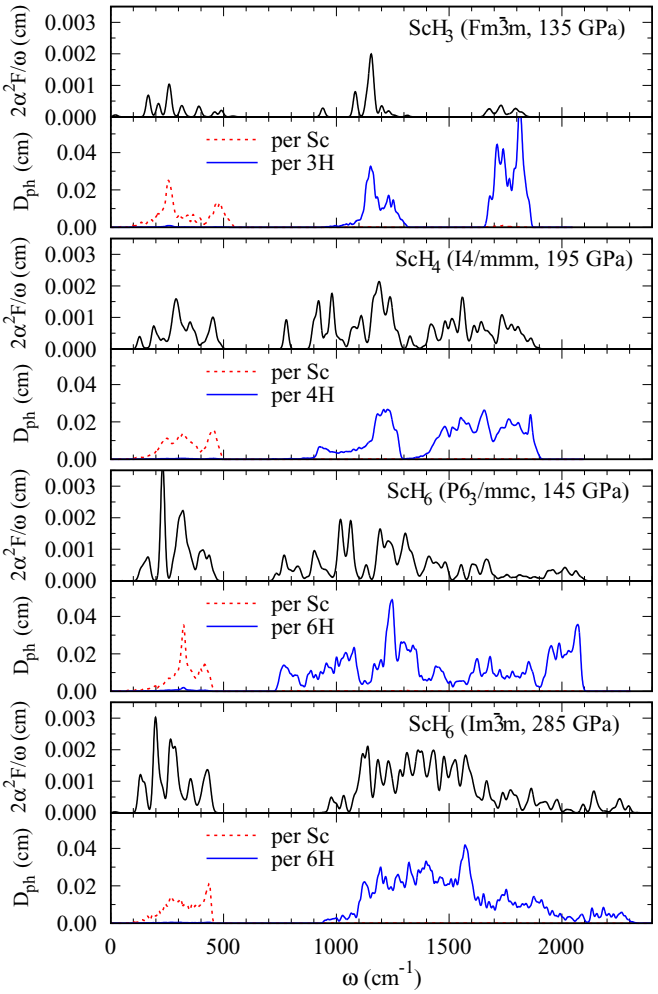

FIG. 5. Eliashberg function α^2F multiplied by $2/\omega$ (i.e. $2\alpha^2F/\omega$) and the density of phonon modes $D_{\rm ph}$ for the $Fm\bar{3}m$ ScH_3 at $r_s = 1.65$ (135 GPa), the $I4/mmm$ ScH_4 at $r_s = 1.55$ (195 GPa), the $P6_3/mmc$ ScH_6 at $r_s = 1.57$ (145 GPa), and the $Im\bar{3}m$ ScH_6 at $r_s = 1.45$ (285 GPa).

V. ELECTRON-PHONON COUPLING

Figure 5 shows the Eliashberg function α^2F multiplied by $2/\omega$ and the density of phonon modes for the ScH_3, ScH_4, and ScH_6 phases. As seen in the density of phonon modes, the continua below $\sim$500 cm^{-1} are made of the phonon modes consisting almost only of Sc motions, and the others at higher frequencies are of H motions. The electron-phonon coupling in the $Fm\bar{3}m$ ScH_3 is quite small even for the Sc phonon modes, which is consistent with the fact that the PDOS of Sc atoms at the Fermi energy comes mostly from the much localized $3d$ states [Fig. 3(a)]. As expected by analogy with the yttrium hydrides, the $I4/mmm$ ScH_4 and the $Im\bar{3}m$ ScH_6 show significant electron-phonon coupling for the entire frequency range. Also, notice that the coupling is still large in the $P6_3/mmc$ hexahydride which is not possible for yttrium.

Table II presents electron-phonon coupling parameter λ, logarithmic average phonon frequency $\omega_{\log}$, and T_c for the two values of μ^* (namely, 0.1 and 0.13), where T_c is calculated by using the McMillan formula with Allen-Dynes corrections [58,59]. The value of T_c in the $Fm\bar{3}m$ ScH_3 is almost zero because of its small λ. This result agrees with a previous work of Kim *et al.* [57], though the pressures considered in their paper are below 80 GPa. In contrast, the ScH_4 and ScH_6 phases possess much larger λ and, accordingly, higher T_c (above 60 K for $\mu^* = 0.13$).

TABLE II. Superconducting properties of the $Fm\bar{3}m$ ScH_3 at $r_s = 1.65$ (135 GPa), the $I4/mmm$ ScH_4 at $r_s = 1.55$ (195 GPa), the $P6_3/mmc$ ScH_6 at $r_s = 1.57$ (145 GPa), and the $Im\bar{3}m$ ScH_6 at $r_s = 1.45$ (285 GPa), where T_c is calculated by using the McMillan formula with Allen-Dynes corrections [58,59].

	P (GPa)	λ	$\omega_{\log}$ (K)	T_c (K)	
				μ^*=1.0	μ^*=1.3
ScH_3 ($Fm\bar{3}m$)	135	0.23	918	0	0
ScH_4 ($I4/mmm$)	195	0.89	1340	81	67
ScH_6 ($P6_3/mmc$)	145	0.95	1110	75	63
ScH_6 ($Im\bar{3}m$)	285	1.33	1300	147	130

Although T_c reaches 130 K in the $Im\bar{3}m$ ScH_6, which is the highest here, the temperature might not look so high if it is compared with those of the $Im\bar{3}m$ phases of YH_6 and CaH_6. Indeed, according to Refs. [26] and [33], the values of T_c are 251 K ($\lambda = 2.93$) in the $Im\bar{3}m$ YH_6 at 120 GPa, and 220 K ($\lambda = 2.69$) in the $Im\bar{3}m$ CaH_6 at 150 GPa, where T_c is estimated by directly solving the Eliashberg equations since λ is too large to apply the extended McMillan formula. The comparatively lower T_c of the $Im\bar{3}m$ ScH_6 is largely due to the pressure range where the phase is stabilized. In fact, the $Im\bar{3}m$ phase has a tendency to give large λ at low pressures, where the phonon modes composed of H motions exhibit substantial softenings. For example, if pressure is lowered to 150 GPa, λ of the $Im\bar{3}m$ ScH_6 increases to 2.15. Around the pressures, however, the lowest-enthalpy structure of ScH_6 is not the $Im\bar{3}m$ but the $P6_3/mmc$. Thus, the stabilization of the $P6_3/mmc$ structure makes the superconducting properties of ScH_6 somewhat different from those of YH_6 and CaH_6, lowering the estimated T_c. Yet, it should be stressed that the T_c value of the $P6_3/mmc$ ScH_6 is still high as phonon-mediated superconductivity. Furthermore, it is quite intriguing to investigate the possibility of the $P6_3/mmc$ hexahydride (or close modifications) for other transition-metal elements. If those polyhydrides are stabilized, much higher T_c is expected because the shift of the Fermi energy can significantly increase the DOS at the Fermi energy [see Fig. 3(c)]. Indeed, such effects of the valence electron number on T_c are well observed in A15-type transition-metal compounds [60], which had been the highest-T_c substances until the mid-1980s [61].

VI. CONCLUSIONS

The possibility of hydrogen-rich compounds of scandium has been investigated by using *ab initio* calculations together with the random structural search method. The calculations have shown that the $I4/mmm$ ScH_4, the $P6_3/mmc$ ScH_6, and the $Im\bar{3}m$ ScH_6 are stabilized above 160, 135, and 265 GPa, respectively. All three phases are metallic, where

the contributions of H orbitals to the DOS at the Fermi energy are clearly observed. Their electronic structures remarkably enhance electron-phonon coupling and raise T_c in comparison with those of the well-known $Fm\bar{3}m$ ScH_3 phase.

The tendency toward metallic polyhydrides at high pressures, which was already predicted with respect to alkaline and alkaline-earth elements, also seems to be the characteristic of group 3 elements. However, there is a difference between scandium and yttrium hydrides, that is, the appearance of the $P6_3/mmc$ ScH_6. Rather, the structural properties found in the hydrides of scandium, yttrium, magnesium, calcium, and so on suggest that there exists the diagonal relationship, which can work as a useful guide in looking for similar hydrides with the shifted Fermi energy. One of the keys to the $P6_3/mmc$ hexahydride is the small size of the hydrogenated atoms. This finding encourages one to investigate nearby d-block elements further since atomic size tends to decrease on moving toward the right side on the periodic table. The consequent shift of the Fermi energy owing to the change of the valence electron number could bring about the increase of the DOS at the Fermi energy and lead to higher T_c. It is also worth noting that metallic polyhydrides were predicted even for a heavy transition-metal element, namely, tungsten [62,63]. Although the DOS at the Fermi energy is small, metallic WH_4 and WH_6 are stabilized above 15 GPa and 150 GPa, respectively. All these findings suggest that the formation of metallic hydrogen-rich compounds and the resulting high-temperature superconductivity are likewise expected extensively for other d-block elements.

Note added. Recently, the author became aware of a theoretical article on scandium hydride by Qian *et al.* [64], where different structural search techniques are used. Together with the phases discussed in the present study, they also proposed a ScH_8 phase with $Immm$ symmetry above 300 GPa.

ACKNOWLEDGMENTS

The author is grateful to O. Yoshida for helpful comments on the manuscript. This work was supported by JSPS KAKENHI (Grant No. 25400353).

[1] N. W. Ashcroft, Phys. Rev. Lett. **21**, 1748 (1968).
[2] J. J. Gilman, Phys. Rev. Lett. **26**, 546 (1971).
[3] N. W. Ashcroft, J. Phys.: Condens. Matter **16**, S945 (2004).
[4] N. W. Ashcroft, Phys. Rev. Lett. **92**, 187002 (2004).
[5] I. Goncharenko, M. I. Eremets, M. Hanfland, J. S. Tse, M. Amboage, Y. Yao, and I. A. Trojan, Phys. Rev. Lett. **100**, 045504 (2008).
[6] M. I. Eremets, I. A. Trojan, S. A. Medvedev, J. S. Tse, and Y. Yao, Science **319**, 1506 (2008).
[7] T. A. Strobel, A. F. Goncharov, C. T. Seagle, Z. Liu, M. Somayazulu, V. V. Struzhkin, and R. J. Hemley, Phys. Rev. B **83**, 144102 (2011).
[8] A. P. Drozdov, M. I. Eremets, I. A. Troyan, V. Ksenofontov, and S. I. Shylin, Nature (London) **525**, 73 (2015).
[9] M. Einaga, M. Sakata, T. Ishikawa, K. Shimizu, M. I. Eremets, A. P. Drozdov, I. A. Troyan, N. Hirao, and Y. Ohishi, Nat. Phys. **12**, 835 (2016).
[10] B. Guigue, A. Marizy, and P. Loubeyre, Phys. Rev. B **95**, 020104(R) (2017).
[11] C. J. Pickard and R. J. Needs, Phys. Rev. Lett. **97**, 045504 (2006).
[12] C. J. Pickard and R. J. Needs, Phys. Rev. B **76**, 144114 (2007).
[13] J. S. Tse, Y. Yao, and K. Tanaka, Phys. Rev. Lett. **98**, 117004 (2007).
[14] M. Martinez-Canales, A. R. Oganov, Y. Ma, Y. Yan, A. O. Lyakhov, and A. Bergara, Phys. Rev. Lett. **102**, 087005 (2009).
[15] G. Gao, A. R. Oganov, P. Li, Z. Li, H. Wang, T. Cui, Y. Ma, A. Bergara, A. O. Lyakhov, T. Iitaka, and G. Zou, Proc. Natl. Acad. Sci. **107**, 1317 (2010).
[16] G. Gao, H. Wang, A. Bergara, Y. Li, G. Liu, and Y. Ma, Phys. Rev. B **84**, 064118 (2011).
[17] P. Zaleski-Ejgierd, R. Hoffmann, and N. W. Ashcroft, Phys. Rev. Lett. **107**, 037002 (2011).
[18] K. Abe and N. W. Ashcroft, Phys. Rev. B **84**, 104118 (2011).
[19] K. Abe and N. W. Ashcroft, Phys. Rev. B **88**, 174110 (2013).
[20] Y. Li, J. Hao, H. Liu, Y. Li, and Y. Ma, J. Chem. Phys. **140**, 174712 (2014).
[21] D. Duan, Y. Liu, F. Tian, D. Li, X. Huang, Z. Zhao, H. Yu, B. Liu, W. Tian, and T. Cui, Sci. Rep. **4**, 6968 (2014).
[22] K. Abe and N. W. Ashcroft, Phys. Rev. B **92**, 224109 (2015).
[23] E. Zurek, R. Hoffmann, N. W. Ashcroft, A. R. Oganov, and A. O. Lyakhov, Proc. Natl. Acad. Sci. USA **106**, 17640 (2009).
[24] P. Baettig and E. Zurek, Phys. Rev. Lett. **106**, 237002 (2011).
[25] D. Zhou, X. Jin, X. Meng, G. Bao, Y. Ma, B. Liu, and T. Cui, Phys. Rev. B **86**, 014118 (2012).
[26] H. Wang, J. S. Tse, K. Tanaka, T. Iitaka, and Y. Ma, Proc. Natl. Acad. Sci. USA **109**, 6463 (2012).
[27] J. Hooper and E. Zurek, Chem. Eur. J. **18**, 5013 (2012).
[28] D. C. Lonie, J. Hooper, B. Altintas, and E. Zurek, Phys. Rev. B **87**, 054107 (2013).
[29] J. Hooper, B. Altintas, A. Shamp, and E. Zurek, J. Phys. Chem. C **117**, 2982 (2013).
[30] J. Hooper, T. Terpstra, A. Shamp, and E. Zurek, J. Phys. Chem. C **118**, 6433 (2014).
[31] Y. Xie, Q. Li, A. R. Oganov, and H. Wang, Acta Cryst. C **70**, 104 (2014).
[32] X. Feng, J. Zhang, G. Gao, H. Liu, and H. Wang, RSC Adv. **5**, 59292 (2015).
[33] Y. Li, J. Hao, H. Liu, J. S. Tse, Y. Wang, and Y. Ma, Sci. Rep. **5**, 9948 (2015).
[34] J. C. McGuire and C. P. Kempter, J. Chem. Phys. **33**, 1584 (1960).
[35] N. F. Miron, V. A. Levdik, V. I. Shcherba, and V. N. Bykov, Sov. Phys. Crystallogr. USSR **16**, 709 (1972).
[36] I. O. Bashkin, E. G. Ponyatovskii, and M. E. Kost, Phys. Status Solidi B **87**, 369 (1978).
[37] I. O. Bashkin, E. G. Ponyatovskii, and M. E. Kost, Inorganic Mater. **14**, 1260 (1978).
[38] V. E. Antonov, I. O. Bashkin, V. K. Fedotov, S. S. Khasanov, T. Hansen, A. S. Ivanov, A. I. Kolesnikov, and I. Natkaniec, Phys. Rev. B **73**, 054107 (2006).
[39] A. Ohmura, A. Machida, T. Watanuki, K. Aoki, S. Nakano, and K. Takemura, J. Alloys Compd. **446**, 598 (2007).

[40] T. Kume, H. Ohura, T. Takeichi, A. Ohmura, A. Machida, T. Watanuki, K. Aoki, S. Sasaki, and H. Shimizu, and K. Takemura, Phys. Rev. B **84**, 064132 (2011).
[41] J. P. Perdew, in *Electronic Structure of Solids '91*, edited by P. Ziesche and H. Eschrig (Akademie Verlag, Berlin, 1991), p. 11; J. P. Perdew, K. Burke, and M. Ernzerhof, Phys. Rev. Lett. **77**, 3865 (1996).
[42] P. Giannozzi, S. Baroni, N. Bonini, M. Calandra, R. Car, C. Cavazzoni, D. Ceresoli, G. L. Chiarotti, M. Cococcioni, I. Dabo, A. Dal Corso, S. de Gironcoli, S. Fabris, G. Fratesi, R. Gebauer, U. Gerstmann, C. Gougoussis, A. Kokalj, M. Lazzeri, L. Martin-Samos, N. Marzari, F. Mauri, R. Mazzarello, S. Paolini, A. Pasquarello, L. Paulatto, C. Sbraccia, S. Scandolo, G. Sclauzero, A. P. Seitsonen, A. Smogunov, P. Umari, and R. M. Wentzcovitch, J. Phys.: Condens. Matter **21**, 395502 (2009).
[43] D. Vanderbilt, Phys. Rev. B **41**, 7892 (1990).
[44] S. Baroni, S. de Gironcoli, A. Dal Corso, and P. Giannozzi, Rev. Mod. Phys. **73**, 515 (2001).
[45] C. J. Pickard and R. J. Needs, J. Phys.: Condens. Matter **23**, 053201 (2011).
[46] The quantity r_s is defined by $v_e = (4\pi/3)r_s^3 a_0^3$, where v_e is the volume per valence electron, and a_0 is the Bohr radius. The number of valence electrons is chosen to be 3 for Sc.
[47] The H-H initial minimum distance is decreased to 1.01 Å for H at $r_s = 1.22$ because the system is very dense.
[48] B. Edwards, N. W. Ashcroft, and T. Lenosky, Europhys. Lett. **34**, 519 (1996).
[49] H. Y. Geng, H. X. Song, J. F. Li, and Q. Wu, J. Appl. Phys. **111**, 063510 (2012).
[50] T. Ishikawa, H. Nagara, T. Oda, N. Suzuki, and K. Shimizu, Phys. Rev. B **90**, 104102 (2014).
[51] K. Nagao, H. Nagara, and S. Matsubara, Phys. Rev. B **56**, 2295 (1997).
[52] B. Cordero, V. Gómez, A. E. Platero-Prats, M. Revés, J. Echeverría, E. Cremades, F. Barragán, and S. Alvarez, Dalton Trans., 2832 (2008).
[53] See, for example, G. Rayner-Canham, Found. Chem. **13**, 121 (2011).
[54] C. J. Pickard and R. J. Needs, Nat. Phys. **3**, 473 (2007).
[55] X. Ye, R. Hoffmann, and N. W. Ashcroft, J. Phys. Chem. C **119**, 5614 (2015).
[56] A. Togo, F. Oba, and I. Tanaka, Phys. Rev. B **78**, 134106 (2008).
[57] D. Y. Kim, R. H. Scheicher, H.-k. Mao, T. W. Kang, and R. Ahuja, Proc. Natl Acad. Sci. USA **107**, 2793 (2010).
[58] W. L. McMillan, Phys. Rev. **167**, 331 (1968).
[59] P. B. Allen and R. C. Dynes, Phys. Rev. B **12**, 905 (1975).
[60] M. Kataoka and N. Toyota, Phase Transitions **8**, 157 (1987).
[61] See, for example, J. Muller, Rep. Prog. Phys. **43**, 641 (1980); D. Dew-Hughes, Cryogenics **15**, 435 (1975).
[62] P. Zaleski-Ejgierd, V. Labet, T. A. Strobel, R. Hoffmann, and N. W. Ashcroft, J. Phys.: Condens. Matter **24**, 155701 (2012).
[63] V. Labet, R. Hoffmann, and N. W. Ashcroft, New J. Chem. **35**, 2349 (2011).
[64] S. Qian, X. Sheng, X. Yan, Y. Chen, and B. Song, Phys. Rev. B **96**, 094513 (2017).